

RSC Advances



This is an *Accepted Manuscript*, which has been through the Royal Society of Chemistry peer review process and has been accepted for publication.

Accepted Manuscripts are published online shortly after acceptance, before technical editing, formatting and proof reading. Using this free service, authors can make their results available to the community, in citable form, before we publish the edited article. This *Accepted Manuscript* will be replaced by the edited, formatted and paginated article as soon as this is available.

You can find more information about *Accepted Manuscripts* in the [Information for Authors](#).

Please note that technical editing may introduce minor changes to the text and/or graphics, which may alter content. The journal's standard [Terms & Conditions](#) and the [Ethical guidelines](#) still apply. In no event shall the Royal Society of Chemistry be held responsible for any errors or omissions in this *Accepted Manuscript* or any consequences arising from the use of any information it contains.

Synthesis of Glycopolymers at Various Pendant Spacer Lengths of Glucose Moiety and Their Effects on Adhesion, Viability and Proliferation of Osteoblast cells

M. Trinadh,^a G. Kannan,^b T. Rajasekhar,^a A. V. Sessa Sainath^{a*} and M. Dhayal^{b*}

^aPolymers and Functional Materials Division, CSIR-Indian Institute of Chemical Technology, Hyderabad 500007, Andhra Pradesh, India.

^bClinical Research Facility, CSIR-Center for Cellular and Molecular Biology, Hyderabad 500007, Andhra Pradesh, India.

*Corresponding authors (Tel: +91 40 27192500, Fax: +91 40 27160591, E-mail: avssainath@yahoo.com (AVSS) and marshal@cmb.res.in (MD)).

Abstract

Multivalent glycopolymers containing three different glucose pendant spacer lengths to the polymer back bone having various weight percentages of covalently bonded glucose moieties were obtained by deacetylation of acetylated polymers synthesized via reversible addition-fragmentation chain transfer (RAFT) process. This allowed us to control the packing density of the glucose moieties in one unit of the glycopolymer. The biological responses of these macromolecules in terms of cytotoxicity of glucose moieties at various spacer length and concentrations were investigated without perturbing the intrinsic chemical nature of functional moiety by employing in vitro osteoblast cells. Osteoblast cells adhesion, viability and proliferation response with synthesized glycopolymers revealed that the glycopolymer concentration tolerance limit was higher with an increase in pendant spacer length of glucose moiety of the glycopolymer.

1. Introduction

The unique properties of glycopolymers which consists of a synthetic polymeric backbone and pendant glyco moieties have been applied in clinical diagnostics, drug and gene delivery systems¹⁻⁶, specific molecular recognition⁷⁻¹⁶, surface modifiers¹⁷⁻¹⁹ and separation of biomolecules²⁰⁻²³. Hence, the interest of researchers have been focused on dealing with the design and development of suitable glycopolymeric materials by tailoring macromolecular chains and test their biological performance. Well defined glycopolymeric materials provide structural and functional support to cells/tissues due to their hydrophilic character, better biocompatibility and ability to mimic glycoproteins in the biological systems.²⁴⁻²⁷ The carbohydrate units in glycopolymers act as ligands in a variety of biological processes and play a significant role in biomolecule recognition and determine the interaction with cells for desirable tissue growth and repair.²⁸⁻³² Moreover, glycans are specific to regulate certain cellular functions of cells due to their multivalent nature and flexibility and varying spatial distribution of glyco moieties in glycans have advantages to develop new materials for biomedical applications.^{33,34} The initial study of Schnaar et al., demonstrated the adhesion of chicken hepatocytes to poly(acrylamide) gels which were derivatized with *N*-acetylglucosamine glycopolymeric coatings.³⁵ The fibroblast cells adhesion and proliferation were carried on hyperbranched glycoacrylate films and glycopolymer coatings on polystyrene carrying *N*-acetylglucosamine residues were studied.^{36,37} The biocompatibility of sugar-modified extra cellular matrices of glycopolymers had been extensively studied by means of liver cells with the variation of carbohydrate moieties to the polymeric backbone architectures.³⁸⁻⁴²

Synthetic glycopolymers are promising as an useful tool which allows a precise control of various biological functions of a cell during cell/surface interactions. The development of new methods for the synthesis of tailor-made glycopolymers as well as glycan derivatives has given access to targeted architectures and modifications with carbohydrate moieties.^{43,44} Previously glucose moiety containing glycopolymer (poly-[3-*O*-(4'-vinylbenzyl)-D-glucose]) was used for culturing erythrocytes and observations confirmed that the presence of reducing glucose moieties was crucial for a specific cell attachment.^{45,46} Despite all of these biologically important functions, there has been a very little attention paid towards the use of glycopolymers having different pendant alkyl chain lengths of glucose functional moiety on polymer backbone in cell and tissue engineering.

To the best of our knowledge, the osteoblast cell adhesion, viability and proliferation with glycopolymers consisting of various pendant alkyl chain of glucose moiety has not been examined yet. However, previously osteoblast cell adhesion to various implant materials such as metal oxides, bioinert metals, metal alloys, bioceramics, synthetic polymers and composites has been extensively studied.⁴⁷⁻⁵⁴ Formerly, poly(pentafluorostyrene)-based glycopolymer coated substrates were used to study the attachment of 3T3 fibroblasts and MC3T3-E1 preosteoblasts.⁵⁵ It is expected that studying osteoblast cells response at various concentrations of glycopolymers having different pendant alkyl chain lengths of glucose functional moieties on acrylate macromolecular chain could help to design bone implant coatings that modulate cell adhesion and proliferation within the multicellular surrounding of the human body. Thus, the study of osteoblast cells interactions with glycopolymers are of great interest for hard tissue engineering and understanding bone formation process.⁵⁶

Here we have used RAFT process for syntheses of glycopolymers containing three different glucose pendant alkyl chain lengths to the polymer back bone. The RAFT process is a commonly used and reliable method for synthesis of glycopolymers to achieve controlled macromolecular architecture from a wide range of functional monomers.⁵⁷⁻⁵⁹ In this paper we report the usefulness of different pendant alkyl chain lengths of functional moiety of glycopolymers to control the response of different cellular functions such as adhesion, viability and proliferation of mouse osteoblast (MC3T3) cells in-vitro.

2. Experimental

2.1 Materials

D-glucose anhydrous (Fisher Scientific Pvt. Ltd.), acetic anhydride and sodium acetate (Sisco Research Laboratories Pvt. Ltd.), benzylamine (Finar Chemicals Limited), methyl ethyl ketone (MEK), acryloylchloride, triethylamine (Et₃N) and azobisisobutyronitrile (AIBN) (Avra Synthesis Pvt. Ltd.), 1,4-butane diol, 1,6-hexane diol, BF₃.Et₂O and 2-cyano-2-propyldodecyltrithiocarbonate (CPDTC) (Sigma-Aldrich) and molecular sieves 4 Å (S d fine-chem limited) were used as received. Dichloromethane (DCM) (Finar Chemicals Ltd) was dried over calcium hydride by stirring over night and distilled. Tetrahydrofuran (THF) (Finar Chemicals Limited) was distilled over sodium wire with benzophenone under nitrogen atmosphere. The osteoblast cells (MC3T3) were obtained from American type culture collection (ATCC), USA and their subclones were maintained in complete medium (CM). The CM was made of fresh α -minimum essential medium (MEM) (Invitrogen, USA) medium having 10% fetal bovine serum (FBS) (Invitrogen, USA) and 100 U/mL penicillin, 50 μ g/mL streptomycin and 50 μ g/mL gentamycin (Invitrogen, USA). The

cells were sub-cultured using trypsin-ethylenediaminetetraacetic acid (EDTA) (Invitrogen, USA).

2.2 Preparation of 1,2,3,4,6-penta-*O*-acetyl-D-glucopyranoside (PAGP)

Well grained mixture of 20 g (0.11 mol) of D-glucose and 25 g (0.304 mol) of sodium acetate was taken in a 500 mL two necked round bottom flask and added 150 mL of acetic anhydride and refluxed for 4 h. After the solution become clear, it was poured back into a conical flask which contained crushed ice. The generated crystals were filtered with a Buckner funnel and dried. Yield: 75%. M.p. 113-5 °C. ¹H NMR (CDCl₃, 300 MHz): δ 5.73 (d, *j* = 7.93 Hz, 1H), 5.26 (m, 1H), 5.14 (t, *j*=9.06, 7.55 Hz, 2H), 4.30 (m, 1H), 4.11 (d, *j*=11.71 Hz, 1H), 3.86 (d, *j*=7.18 Hz, 1H) and 2.09-2.02 (m, 15H). ESI-MS: *m/z*: 413 (M + Na)⁺. IR (KBr, cm⁻¹): ν 2969 (-CH-), 1746 (-O-C=O-), 1375 (-O-C-, ester) and 1226 (-C-O-C-).

2.3 Preparation of 2,3,4,6-tetra-*O*-acetyl-D-glucopyranoside (TAGP)

A solution of PAGP (5.0 g, 0.0128 mol) and benzyl amine (2.1 mL, 0.0192 mol) in 30 mL of THF was taken in 100 mL two necked round bottom flask and stirred over night at room temperature.⁶⁰ The mixture was diluted with cold water and extracted with chloroform (3×200 mL). The extracted layer was successively washed with ice cold dilute HCl solution, saturated NaHCO₃ solution, saturated NaCl solution and water. The mixture was dried over anhydrous Na₂SO₄ and concentrated in vacuum. The residue was purified by column chromatography technique with ethyl acetate and *n*-hexane (2/3, v/v) mixture to give 3.5 g of TAGP. The TAGP is a viscous liquid. Yield: 80%. ¹H NMR (CDCl₃, 300 MHz): δ 5.55 (t, *j*=9.44 Hz, 1H), 5.43 (s, 1H), 5.07 (t, *j*=9.06 Hz, 2H), 4.87 (d, *j*=9.44 Hz, 1H), 4.37 (s, 1H), 4.24 (m, 1H), 4.08 (s, 1H) and 2.17-2.01 (m, 12H). ESI-MS: *m/z*: 371 (M + Na)⁺. IR (KBr, cm⁻¹): ν 3328 (-OH), 2956 (-CH-), 1750 (-O-C=O-), 1432, 1370 (-O-C-, ester) and 1231 (-C-O-C-).

2.4 Synthesis of 4-hydroxybutyl acrylate (HBA)

The HBA was prepared as reported in literature.⁶¹ The 1,4-butanediol (26.9 g, 0.299 mol) was reacted with acryloylchloride (6.92 g, 0.0765 mol) in the presence of triethylamine (10.9 g, 0.108 mol). The obtained mixture was purified by column chromatography using hexane/ethyl acetate (v/v, 1/1) as eluent. The HBA was liquid in nature. ¹H NMR (CDCl₃, 300 MHz): δ 6.40 (d, *j*=17.18 Hz, 1H), 6.20-6.03 (m, 1H), 5.82 (d, *j*=10.39 Hz, 1H), 4.19 (m, 2H), 3.67 (m, 2H) and 1.88-1.54 (m, 4H). ESI-MS: *m/z*: 145 (M + H)⁺. IR (KBr, Cm⁻¹): ν 3425 (-OH), 2951 (-CH-), 1723 (-O-C=O-), 1410, 1370 (-O-C-, ester) and 1194 (-C-O-C-).

2.5 Preparation of 6'-hydroxyhexyl-2,3,4,6-tetra-O-acetyl-D-glucopyranoside (HHTAGP)

A solution of PAGP (10 g, 0.026 mol) in dichloromethane (80 mL) was stirred for 2 h with molecular sieves (4 g, 0.4 mm) under nitrogen atmosphere.⁶² Then the BF₃.Et₂O (6.5 mL, 0.051 mol) was subsequently added to the mixture and immediately 1,6 hexane diol (3.32 g (0.028 mol) in 15 mL dichloromethane) was added. After 10 days, the mixture was poured into saturated NaHCO₃ solution (100 mL). The organic layer was separated and the aqueous phase was extracted with dichloromethane for 3 times, each time with 40 mL. The collected organic phase was washed twice with water, each time with 40 mL. Dichloromethane was evaporated in vacuum and the resulting syrup was purified by column chromatography (hexane/ethylacetate (7/3, v/v)). The HHTAGP is a viscous liquid. Yield: 40%. ¹H NMR (CDCl₃, 300 MHz): δ 5.55-5.32 (d, *j*=32.86 Hz, 1H), 5.15-4.92 (m, 2H), 4.87-4.72 (d, *j*=11.71 Hz, 1H), 4.36-4.16 (d, *j*=11.71 Hz, 1H), 4.14-3.88 (m, 4H), 3.76-3.61 (broad s, 1H), 3.52-3.34 (broad s, 1H), 2.24-1.88 (m, 12H) and 1.73-1.15 (m, 8H). ESI-MS: *m/z*: 471 (M + Na)⁺. IR (KBr,

cm⁻¹): ν 3328 (-OH), 2956 (-CH-), 1750 (-O-C=O-), 1432, 1370 (-O-C-, ester) and 1231 (-C-O-C-).

2.6 Preparation of glycoacrylates Acryl-2,3,4,6-tetra-*O*-acetyl-D-glucopyranoside (ATAGP) and 6'-(acryloxy)hexyl-2,3,4,6-tetra-*O*-acetyl-D-glucopyranoside (AHTAGP)

The ATAGP and AHTAGP were synthesized according to a typical standard procedure as follows. A solution of the TAGP (18 g, 0.0517 mol) in 180 mL of MEK and 14.39 mL (0.1035 mol) of triethylamine was taken in a 500 mL two necked round bottom flask equipped with a magnetic stirrer and placed in an ice bath. Acryloylchloride (5.55 mL (0.0568 mol) in 25 mL of MEK) was added drop by drop with constant stirring without raising the temperature above 0 °C. The reaction mixture was stirred for period of 5 h after removing the ice bath. The quaternary ammonium salt (precipitate) was filtered. The supernatant was washed with cold distilled water and dried with anhydrous Na₂SO₄. The ATAGP was isolated by evaporating the solvent and purified by column chromatography technique. The ATAGP was a viscous liquid in nature. Yield: 75%. ¹H NMR (CDCl₃, 300 MHz): δ 6.59-6.35 (m, 1H), 6.25-6.03 (m, 1H), 6.01-5.90 (t, $j=10.20$, 1H), 5.81-5.71 (d, $j=7.93$, 1H), 5.53-5.41 (t, $j=9.82$, 1H), 5.30-5.06 (m, 1H), 4.33-4.19 (m, 1H), 4.17-3.99 (d, $j=3.40$ Hz, 1H), 3.92-3.79 (d, $j=7.93$ Hz, 1H) and 2.12-1.87 (m, 12H). ¹³C NMR (CDCl₃, 75 MHz): δ 20.24, 20.37, 20.41, 20.51, 61.31, 67.68, 67.80, 69.10, 69.76, 70.05, 72.55, 72.61, 89.18, 91.81, 132.92, 133.34, 163.61, 169.07, 169.23, 169.53, 169.89, 170.0 and 170.42. ESI-MS: m/z : 425 (M + Na)⁺. IR (KBr, cm⁻¹): ν 2963 (-CH-), 1750 (-O-C=O-), 1634 (-C=C-), 1409, 1370 (-O-C-, ester) and 1221 (-C-O-C-). AHTAGP: Yield: 75%, viscous liquid. ¹H NMR (CDCl₃, 500 MHz): δ 6.47-6.36 (d,

$j=17.0$ Hz, 1H), 6.19-6.05 (m, 1H), 5.82-5.78 (d, $j=10.58$ Hz, 1H), 5.27-5.15 (t, $j=9.44$ Hz, 1H), 5.15-5.04 (m, 1H), 5.04-4.92 (m, 1H), 4.52-4.46 (d, $j=7.93$ Hz, 1H), 4.32-4.22 (m, 4H), 4.20-4.08 (d, $j=7.18$ Hz, 1H), 3.94-3.81 (m, 1H), 3.76-3.64 (d, $j=9.44$ Hz, 1H), 3.55-3.41 (m, 1H), 2.15-2.19 (m, 12H), 1.73-1.50 (m, 4H) and 1.45-1.29 (s, 4H). ^{13}C NMR (CDCl_3 , 75 MHz): δ 20.35, 20.47, 61.27, 67.64, 69.06, 69.67, 70.01, 72.47, 72.54, 91.74, 126.87, 133.29, 163.56, 169.01, 169.18, 169.83 and 170.34. ESI-MS: m/z : 525 ($\text{M} + \text{Na}$) $^+$. IR (KBr, cm^{-1}): ν 2962 (-CH-), 1745 (-O-C=O-), 1633 (-C=C-), 1409, 1376 (-O-C-, ester) and 1230 (-C-O-C-).

2.7 Preparation of 4'-(acryloxy)butyl-2,3,4,6-tetra-O-acetyl-D-glucopyranoside (ABTAGP)

The PAGP (10 g, 0.026 mol) and 4-hydroxybutylacrylate (3.32 g, 0.023 mol) were dissolved in 70 mL of DCM and subsequently, $\text{BF}_3 \cdot \text{Et}_2\text{O}$ (10.92 g, 0.077 mol) was added *via* syringe. The mixture was sonicated for 45 min. The reaction mixture was washed with brine (saturated solution) and the organic layer was dried over MgSO_4 . After removing the solvent under reduced pressure, the yellow syrup was purified by flash column chromatography using hexane and ethylacetate mixture (7/3, v/v). Yield: 45%. ^1H -NMR (CDCl_3 , 500 MHz): δ 6.47-6.40 (dd, $j=1.07$ Hz, 1H), 6.16-6.06 (m, 1H), 5.93-5.88 (dd, $j=1.07$ Hz, 1H), 5.58-5.51 (t, $j=9.77$ Hz, 1H), 5.15-5.06 (m, 2H), 4.96-4.91 (dd, $j=3.66$ Hz, 1H), 4.31-4.17 (m, 2H), 4.16-3.99 (m, 4H), 3.77-3.69 (m, 1H), 3.51-3.39 (m, 1H), 2.09-1.97 (m, 12H), 1.81-1.53 (m, 2H) and 1.31-1.20 (m, 2H). ^{13}C NMR (CDCl_3 , 75 MHz): δ 20.59, 20.91, 25.27, 25.80, 29.64, 61.37, 61.96, 63.95, 67.24, 67.78, 68.10, 68.46, 69.21, 69.82, 70.07, 70.53, 70.96, 72.68, 95.70, 127.37, 132.41, 165.09, 169.56, 170.17, 170.63 and 171. IR (KBr, cm^{-1}): ν 2949 (-CH-), 1750 (-O-C=O-), 1634 (-C=C-), 1409, 1369 (-O-C-, ester) and 1227 (-C-O-C-).

2.8 Polymerization

All the monomers, ATAGP, AHTAGP and ABTAGP were polymerized *via* RAFT method. Typical ATAGP polymerization procedure was as follows. A mixture of acryl-2,3,4,6-tetra-*O*-acetyl-D-glucopyranoside (1.7 g, 0.0042 mol), AIBN (18 mg, 0.00012 mol) and RAFT agent, CPDTC (58 mg, 0.00016 mol) in 20 mL of THF was deoxygenated by three times of freeze and thaw cycles. Then, the flask was sealed and heated to 80 °C under stirring. It was allowed for 30 h. After that, the polymerization was stopped by the addition of 0.5 mL of methanol and exposed to air. The polymer was isolated by 2-fold precipitation in cold methanol and one time in 30% mixture of ethyl acetate in hexane. The yield of poly(acryl-2,3,4,6-tetra-*O*-acetyl-D-glucopyranoside) (P(ATAGP)) was about 55%. P(ATAGP): ^1H NMR (CDCl_3 , 300 MHz): δ 6.40-6.16, 5.80-5.57, 5.52-5.35, 5.34-5.20, 5.19-4.68, 4.51-4.18, 4.17-3.98, 3.96-3.72, 2.73-2.24, 2.21-1.82, 1.79-1.06 and 0.90-0.75. ^{13}C NMR (CDCl_3 , 75 MHz): δ 67.73, 69.77, 70.12, 72.70, 89.17, 89.65, 169.23, 169.32, 169.98, 170.47 and 170.56. IR (KBr, cm^{-1}): ν 2962 (-CH-), 1756 (-O-C=O-), 1634 (-C=S-), 1439, 1374 (-O-C-, ester) and 1226 (-C-O-C-). Poly(4'-(acryloxy)butyl-2,3,4,6-tetra-*O*-acetyl-D-glucopyranoside) (P(ABTAGP)): Yield : 46%. ^1H NMR (CDCl_3 , 300 MHz): δ 6.47-6.16, 5.89-5.56, 5.53-5.37, 5.37-5.25, 5.25-4.90, 4.56-4.23, 4.20-4.01, 3.98-3.82, 2.85-2.29, 2.26-1.78, 1.56-0.95 and 0.92-0.82. ^{13}C NMR (CDCl_3 , 75 MHz): δ 20.68, 61.09, 65.11, 67.64, 69.24, 69.62, 72.35, 72.58, 72.67, 89.17, 169.00, 169.17, 169.37, 169.90 and 169.98. IR (KBr, cm^{-1}): ν 2962 (-CH-), 1755 (-O-C=O-), 1635 (-C=S-), 1437, 1371 (-O-C-, ester) and 1226 (-C-O-C-). Poly(6'-(acryloxy)hexyl-2,3,4,6-tetra-*O*-acetyl-D-glucopyranoside) (P(AHTAGP)): Yield: 68%. ^1H NMR (CDCl_3 , 300 MHz): δ 6.40-6.24, 5.84-5.59, 5.53-5.37, 5.37-5.21, 5.21-4.95, 4.48-4.20, 4.20-4.03, 3.99-

3.79, 3.76-3.54, 2.74-2.25, 2.19-1.94, 1.93-1.92 and 0.93-0.81. ^{13}C NMR (CDCl_3 , 75 MHz): δ 20.45, 68.26-67.27, 70.46-69.60, 72.61, 91.75, 169.11, 169.32, 169.30, 170.51 and 170.61. IR (KBr, cm^{-1}): ν 2963 (-CH-), 1756 (-O-C=O-), 1634 (-C=S-), 1437, 1372 (-O-C-, ester) and 1226 (-C-O-C-).

2.9 Deacetylation of pendant 2,3,4,6-tetra-O-acetyl-D-glucopyranoside moieties

The deacetylated polymers, poly(acryl-D-glucopyranoside) (**GP1**), poly(4-(acryloxy)butyl-D-glucopyranoside) (**GP2**) and poly(6-(acryloxy)hexyl-D-glucopyranoside) (**GP3**) were synthesized according to a typical procedure as follows.

The P(ATAGP) (200 mg) was dissolved in anhydrous methanol and chloroform (2:1) (total volume: 10 mL) and allowed stirring under nitrogen atmosphere. A solution of NaOMe (101 mg) in anhydrous methanol (2 mL) was added through a syringe and the reaction mixture was left stirring for 90 min. Then solvent was removed by vacuum evaporation and neutralized with 2M HCl solution by stirring over night. After that, the solution was passed through the basic alumina to neutralize the solution. Excess water was removed by lyophilisation, and the polymer was recovered as a white powder by precipitation in excess acetone. **GP1**: IR (KBr, cm^{-1}): ν 3425 (-OH-), 2927 (-CH-), 1735 (-O-C=O-), 2200 (-CN) and 1628 (-C=S-). **GP2**: IR (KBr, cm^{-1}): ν 3416 (-OH-), 2962 (-CH-), 1750 (-O-C=O-), 2200 (-CN) and 1620 (-C=S-). **GP3**: IR (KBr, cm^{-1}): ν 3425 (-OH-), 2927 (-CH-), 1755 (-O-C=O-), 1635 (-C=S-), 1430, 1383 (-O-C-, ester) and 1239 (-C-O-C-).

2.10 Estimation of covalently bonded glucose moiety weight percentage in glycopolymer

Covalently bonded glucose moiety in glycopolymer was calculated to determine their packing density in one unit of glycopolymer. The degree of polymerization (Dp) of glycopolymer was estimated using equation 1.

$$D_p = \left[\frac{\{G_p(M_w) - 345\}}{M(F_w)} \right] \text{----(1)}$$

Where, $G_p(M_w)$: molecular weight of deacetylated glycopolymer by ^1H NMR, $M(F_w)$: deacetylated monomer formula weight and 345 is a constant representing molecular weight of terminal ends of macromolecular chain generated by RAFT agent. Hence, glucose moiety (G_M) wt% was calculated using equation 2.

$$G_M(\text{wt}\%) = 100 \times D_p \left[\frac{G_M(F_w)}{G_p(M_w)} \right] \text{----(2)}$$

Where, $G_M(F_w)$ is glucose moiety formula weight. All three glycopolymers covalently bonded glucose moiety weight percentages were calculated using the above equations.

2.11 In vitro cell assays

Cell culture and statistical analysis: The adherent osteoblast cells (MC3T3) were maintained in culture medium (CM) at 37 °C in 5% CO₂. The CM was prepared using α -MEM medium, supplemented with 10% FBS and 100 U/mL penicillin, 50 $\mu\text{g}/\text{mL}$ streptomycin and 50 $\mu\text{g}/\text{mL}$ gentamycin. The cells were sub-cultured after reaching 80% confluency using trypsin-EDTA. In a 96 well plate, 10^4 cells were plated in each well and different concentrations of glycopolymer were added to the cells. The stock solution of different concentrations of all three glycopolymers were prepared in phosphate buffered saline (PBS) and sterilized by autoclaving at 121.5 °C for 20 mins. Final concentrations of the glycopolymer ranging from 1 nM to 10000 μM were achieved by adding 4 μL of stock solution of different desired concentration in 96 μL of CM for each set of experiments. Separate stock solutions of the glycopolymers were

prepared for each concentration and it was in such a manner that only 4 μL of solution was added to achieve all the desired final concentrations. All cell culture experiments were done in triplicates with cells not exceeding ten passages post revival. The statistical analysis for *in vitro* cell assay was done, based on three experiments for each condition in which minimum three samples were used. Microsoft excel software was used for calculating mean and standard deviation values for all assays.

Cell adhesion assay: This assay was carried out by plating similar number of cells in the plastic tissue culture plate wells. After 4 h, non adherent cells were washed off and 10 μL of 2 mg/mL MTT (3-(4,5-dimethylthiazol-2-yl)-2,5-diphenyltetrazolium bromide) was added to the remaining cells of each condition followed incubation at 37 $^{\circ}\text{C}$ and 5% CO_2 for 4 h. After removing CM, the reaction was stopped by adding dimethylsulfoxide and read at 595 nm in ELISA reader.

Cell viability assay: The assay was performed by plating similar number of cells of all conditions in triplicates and incubated. After 24 h of incubation, MTT assay was performed as described above to calculate the percentage of cell viability.

Cell proliferation assay: The assay was performed by plating similar number of cells of all conditions in triplicates and incubated at dissimilar time periods namely, 4, 24, 48 and 72 h. At the specified time periods cell number at each concentration was calculated by MTT assay as described above.

Immunofluorescence staining: Different concentrations of glycopolymer were added to the cells plated in 6 well plate and incubated for up to 24 h. After this the cells were fixed with 4% formaldehyde (Sigma, USA) for 5-6 min. Cells were washed with PBS for 3 times and permeabilization was done with 0.1% Triton X-100 for 5-6 min following 3 times washing with PBS. Blocking was done with 3% bovine serum albumin (BSA) for 1 h, and cells were washed with PBS once. Rodamine-phalloidin

(Molecular Probes, USA) diluted in 1% BSA to 1:200 ratio was added to the cells and incubated for 1 h. Finally cells were washed once with PBS and mounted using fluoroshield 4',6-diamidino-2-phenylindole (DAPI) (Sigma, USA). Cells were imaged with fluorescent microscope (Axio Imager.Z1, Carl Zeiss, Jena Germany). Integrin $\alpha 5$ and talin co-staining has been carried out as follow, after 24hrs cells on the above substrates were fixed in 4% paraformaldehyde for 10 min at room temperature, permeabilized with 0.1% Triton-X-100 for 10 min and blocked with 3% BSA (Bovine Serum Albumin, Sigma) for 30 min. The cells were treated with rabbit anti-mouse integrin $\alpha 5$ antibody at 1:200 (Santa Cruz, USA) for 1 h at room temperature followed by 1 h incubation with goat anti-rabbit FITC (Fluorescein isothiocyanate) at 1:200 (GeneI, Bangalore, India). Same procedure and conditions repeated for talin staining with mouse anti-mouse talin antibody followed by a 1 h incubation with goat anti-mouse TRITC in the dark at room temperature. Images of cells were captured using a 40x and 63x objective in an AxioVision imaging system (Zeiss, Germany).

2.12 Measurements

The FT-IR (Thermo Nicolet Nexus 670 spectrometer) spectra were recorded at a resolution of 4 cm^{-1} using KBr optics at room temperature and a minimum of 32 scans were signal averaged. The proton nuclear magnetic resonance (^1H NMR) and carbon nuclear magnetic resonance (^{13}C NMR) spectra were recorded on AVANCE-300 or INOVA-500 spectrometer in CDCl_3 or D_2O (Aldrich) depends on the solubility of the products with tetramethylsilane as an internal standard. Mass spectra were recorded on FINNGAN LCQ Advance Max in methanol. Gel permeation chromatography (GPC) was performed by using a Shimadzu system built-in with one (300 \times 7.5 mm) PLgel 5 μm 10E3 Å column (VARIAN) and evaporative light-scattering (PL-ELS) detector (Polymer Laboratories). The eluent was DMF with a flow rate of 0.5 mL min^{-1} at 30

°C. Calibration for detector response was gained using a single narrow PS standard (molecular weights: 550, 1,480; 3,950; 10,680 and 31,420 from Polymer Labs). 1 mg of polymer was dissolved in 1 mL of DMF. Values of M_n and M_w/M_n were determined using LC Solution for Windows software. CO₂ incubator was purchased from Thermo Scientific, USA. Spectrophotometric measurements of adhesion and proliferation were taken from Molecular Devices – Spectra Max – 190, USA.

3 Results and discussion

3.1 Glycopolymers characterization

The synthesized glycoacrylates, acryl-2,3,4,6-tetra-*O*-acetyl-D-glucopyranoside (ATAGP), 4'-(acryloxy)butyl-2,3,4,6-tetra-*O*-acetyl-D-glucopyranoside (ABTAGP) and 6'-(acryloxy)hexyl-2,3,4,6-tetra-*O*-acetyl-D-glucopyranoside (AHTAGP) were polymerized by RAFT process using 2-cyano-2-propyldodecyltrithiocarbonate as RAFT agent with azobisisobutyronitrile as a radical initiator to produce homopolymers, poly(acryl-2,3,4,6-tetra-*O*-acetyl-D-glucopyranoside) (poly(ATAGP)), poly(4'-(acryloxy)butyl-2,3,4,6-tetra-*O*-acetyl-D-glucopyranoside) (poly(ABTAGP)) and poly(6'-(acryloxy)hexyl-2,3,4,6-tetra-*O*-acetyl-D-glucopyranoside) (poly(AHTAGP)) with dodecyl alkyl terminal end, respectively. The resulted polymers pendant 2,3,4,6-tetra-*O*-acetyl-D-glucopyranoside units were deacetylated in the presence of sodiummethoxide/chloroform/methanol mixture to obtain the poly(acryl-D-glucopyranoside) (**GP1**), poly(4-(acryloxy)butyl-D-glucopyranoside) (**GP2**) and poly(6-(acryloxy)hexyl-D-glucopyranoside) (**GP3**) glycopolymers, respectively. The structures of the polymers before and after deacetylation are shown in Scheme 1.

After deacetylation, number average molecular weights (M_n), 10829, 9856 and 4266 g/mol for **GP1**, **GP2** and **GP3**, respectively with M_w/M_n : ~ 1.15 (Table 1) were obtained by gel permeation chromatography studies in DMF with polystyrene standards. The deacetylated glycopolymers, **GP1**, **GP2** and **GP3** were soluble in water which were insoluble prior to deacetylation. Acetylated polymers pendant 2,3,4,6-tetra-*O*-acetyl signals integrations of the glucose moieties showed at δ 1.8-2.3 ppm in ^1H NMR spectra as shown in Fig. 1a. The polymers after deacetylation, the acetyl peaks disappeared and new signals corresponding to OH groups of the glucose moieties⁶³ emerged at δ 3.8–3.92 ppm (Fig. 1b).

The FT-IR analyses of poly(ATAGP), poly(ABTAGP) and poly(AHTAGP) exhibited the characteristic strong absorptions for C=O stretching centred at about 1756 cm^{-1} while the **GP1**, **GP2** and **GP3** showed that the C=O stretching peak shifted to 1735 cm^{-1} with lower intensities (ESI Fig. S7 and S8). The OH signals of the **GP1**, **GP2** and **GP3** showed characteristic strong absorption centred at 3425 cm^{-1} . After deacetylation, the glass transition temperature values of the polymers were decrease in the range of $63\text{-}85^\circ\text{C}$ as shown in Table 1.

3.2 Cell adhesion

Fig. 2 shows cell adhesion on tissue culture plastic (TCP) surfaces at various concentrations (100 nM, 1 μM , 10 μM and 100 μM) of **GP1**, **GP2** and **GP3** in the cell culture media. To carry out quantitative analysis of adhesion % of osteoblast cells, we have used colorimetric cell-surface adhesion assay in which cells were incubated with MTT after 4 h of cell adhesion on surface. Non-adhered cells were washed out by removing the culture media. Dimethylsulfoxide was added to the surface adhered cells and then, the absorbance was measured at 595 nm as disrobed previously.⁵¹ This method has been well accepted for measuring number of adherent cells.⁶⁴

The use of **GP1** at various concentrations did not exhibit any significant change on osteoblast cell adhesion. However, the % of cell adhesion was a little less than the cell adhesion was achieved on TCP without the use of **GP1**. The use of **GP3** at 100 μM concentration had shown increased about 6% cell adhesion compared to the **GP2**. Fig. 3 shows cell adhesion on TCP surfaces at higher concentrations (10 μM to 2000 μM) of **GP1**, **GP2** and **GP3** and these results were compared with the absence of glycopolymers. It has been shown that the use of 10 and 100 μM of **GP1** and **GP2** did not exhibit any significant change on osteoblast cells adhesion. However, a further increase in the concentration (1000 and 2000 μM) of **GP1** and **GP2** showed rapid decrease in the osteoblast cells adhesion. On the other hand, the **GP3** which has largest pendant alkyl chain length of glucose moiety in glycopolymer showed relatively better osteoblast cells adhesion at similar concentrations of the **GP1** and **GP2**.

These observations clearly indicate that the decrease in pendant alkyl chain length of glucose moiety in glycopolymer can reduce cell adhesion at higher concentrations. To have better understanding about the role of pendant alkyl chain length of glucose moiety on osteoblast cells, an estimation of glucose moiety weight percentage (wt%) in each glycopolymer were calculated from ^1H NMR (see in experimental, equation 1 and 2). The increase in the pendant spacer length (0, 4 and 6 alkyl chain length) of glycopolymer has decreased the covalently bonded glucose moiety packing density in glycopolymer (71, 56 and 48 wt%, respectively). Hence, cell adhesion was plotted with varying covalently bonded glucose moiety concentration in glycopolymers (ESI, Fig. S11). The **GP1** and **GP2** exhibited similar osteoblast cells adhesion until 300 μM concentration of covalently bonded glucose moiety and a further increase in the concentration showed decrease in the osteoblast cells adhesion. Whereas, the **GP3**, which has the largest pendant alkyl chain length of glucose moiety in glycopolymer,

showed relatively better osteoblast cells adhesion at similar concentrations of covalently bonded glucose moiety of the **GP1** and **GP2**. To further validate above results, free glucose (**FG**) at various concentrations was added to the culture media and there was no significant different on cells adhesion was observed while increasing the **FG** concentration (ESI, Fig. S11).

3.3 Immunofluorescence staining

It is well establish fact that the cell spreading and movement occur though the process of binding of cell surface integrin receptors to extracellular matrix adhesion molecules. The complex at the focal adhesions consists of several proteins such as vinculin, talin, α -actin and paxillin at the intracellular face of the plasma membrane. Thus, to have better understanding of cell adhesion and understanding cytoskeletal organization integrin α 5 and talin co-stained microscopic image of osteoblast cell on tissue culture plastic surfaces at various concentrations of all three glycopolymers were obtained. Talin and integrin α 5 immunostaining were performed at 1 μ M of **GP1**, **GP2** and **GP3** and cell cytoskeletal organization was compared with control, without the use of glycopolymer on tissue culture plastic surfaces, as shown in Fig. 4. From the observations, it was clearly indicative that cells spreading were well in the presence of different glycopolymers and relative number of the focal contact points were decreased with increase in pendant spacer length of glucose moiety in glycopolymers from **GP1** to **GP3**. Merged immunostained images clearly showed that talin co-localized with integrin α 5. The integrin α 5 staining images showed functional role of the cytoplasmic domain of the alpha subunit of the integrin which play an important role in determining cell surface interaction.⁶⁵ Optical images of the cells at 1 μ M of **GP1**, **GP2** and **GP3** were obtained and are shown in Fig. 5. Decrease in the number of cells was observed with increasing of glycopolymers concentrations (ESI, Fig. S12).

To investigate cell motility and cytoskeletal organization at various concentrations of **GP1**, **GP2** and **GP3**, integrin $\alpha 5$ and talin immunostaining were performed and the results are shown in ESI, Fig. S13-15, respectively. A significant difference was observed at various concentrations of glycopolymer while increasing the pendant spacer length of glucose moiety in glycopolymers. The **GP2** (ESI, Fig. S14) and **GP3** (ESI, Fig. S15) were shown better cell spreading as compared to the **GP1** (ESI, Fig. S13) at similar concentrations.

Actin staining on TCP was used for qualitative analysis of cells spreading in terms of cytoskeleton protein expression at various concentrations of **GP1**, **GP2** and **GP3** and the results are shown in Fig. 6. These observations clearly indicate that the increasing concentration of glycopolymers have effects on cell morphology and spreading. The use of low concentrations ($<100 \mu\text{M}$) of all three glycopolymers did not exhibit any observable differences in actin staining and the results were similar to the staining obtained on TCP without glycopolymers (ESI, Fig S16). Concentrations at and above $1000 \mu\text{M}$ of **GP1** and **GP2** had showed reduced focal contact points which leads to shrinkage in the size of cells. Whereas the obtained microscopic actin stained cell images at higher concentrations (up to $2000 \mu\text{M}$) of the **GP3** had maintained significantly good number of focal points, hence no shrinkage in the size of cells was observed. Integrin $\alpha 5$ and talin staining on TCP at higher concentrations of glycopolymers were obtained and a significant reduction was observed in cell spreading. Similar results were observed for integrin $\alpha 5$ and talin for the use of glycopolymers at higher concentrations and a representative result of immune stained osteoblast cell at $1000 \mu\text{M}$ of **GP3** was given in supporting information (ESI, Fig 17).

3.4 Osteoblast cell viability and proliferation

There were no significant difference in cell viability was observed at the lower concentrations of covalently bonded glucose moiety of **GP1** and **GP3** as compared to the cells viability (~70%) without the use of the glycopolymers (Fig. 7). The **GP2** showed higher cell viability (~95%) for the use of concentrations up to 300 μM as compared to the cell viability obtained for **GP1** and **GP3**. A further increase (>300 μM) in the concentration of covalently bonded glucose moiety of **GP1** and **GP2** showed a steep decrease in cell viability. However the use of the **GP3** at concentrations above 300 μM showed relatively slow decrease in the cells viability. The osteoblast cells were able to maintain their normal viability at higher concentrations (up to 2000 μM) for the use of covalently bonded glucose moiety of **GP3**, which has the largest pendant alkyl chain length of the glucose moiety compared to the **GP1** and **GP2**.

Osteoblast cells proliferation was estimated at 24, 48 and 72 h after plating the cells at various concentrations (0-3000 μM) of covalently bonded glucose moiety of glycopolymers and results are shown in Fig. 8. At lower concentrations (0 to 300 μM), the cell proliferation did not exhibit any significant difference with variation in alkyl chain length of glucose moiety in glycopolymers. The cell proliferation was reduced rapidly with a further increase in concentration of covalently bonded glucose moiety of the **GP1** and **GP2** and most of the cells had lost their viability at 1000 μM concentration. Interestingly, we have not observed any adverse effects on osteoblast cell viability at 2000 μM concentration of covalently bonded glucose moiety of **GP3**.

As per our knowledge and available literature, this is the first report in which the effects of covalently bonded spacer length of glucose in glycopolymer on osteoblast cells have been investigated. However, previous studies have shown the improved cell response on metal surfaces having micro/nano-topography and polymeric scaffolds at

in-vitro and *in-vivo* conditions.⁶⁶⁻⁷⁰ Hence we expect to use this macromolecular architecture design for developing glycopolymers coatings on metal implants in the future.

Conclusions

In conclusion, glycopolymers were synthesized by introducing different alkyl chain spacer lengths between glucose moiety and polymer back bone and dodecyl alkyl chain at one terminal end of the macromolecular chain *via* the RAFT process. The effects of pendant spacer lengths of functional moieties in glycopolymers on osteoblast cells adhesion, viability and proliferation were investigated. It was demonstrated that compatibility of cytotoxicity limits of osteoblast cells depend on pendant spacer length of glucose moieties in glycopolymer. Among the synthesized glycopolymers, the glycopolymer with six pendant spacer lengths of glucose moiety exhibited better osteoblast cell adhesion and proliferation at relatively higher concentrations. These glycopolymers may have the potential role in orthopaedic applications as a biologically active coating material on implants.

Acknowledgements

AVSS and MD thank the Council for Scientific and Industrial Research, India for financial support in network projects CSC 0134 and BSC-0112, respectively. We thank CSIR-CCMB microscopy facility. MT, TR and GK thank CSIR, UGC and CSIR network project for providing fellowships, respectively. MD is thankful to Mr. N R Chakravarthi, Microscopy Facility of CCMB for his help in obtaining brightfield images of cells.

Supplementary Information:

Electronic Supplementary Information (ESI) for detailed characterisation of glycopolymer and cellular response of free glucose are available: [details of any supplementary information available should be included here]. See DOI: 10.1039/b000000x/.

References

- 1 E. Palomino, *Adv Drug Deliv Rev.*, 1994, **13**, 311–323.
- 2 X. M. Chen, J. S. Dordick and D. G. Rethwisch, *Macromolecules*, 1995, **28**, 6014–6019.
- 3 J. Li, S. Zacharek, X. Chen, J. Wang, W. Zhang, A. Janczuk and P. G. Wang, *Bioorg. Med. Chem.*, 1999, **7**, 1549–1558.
- 4 M. G. Garcia-Martin, C. Jimenez-Hidalgo, S. S. J. Al-Kass, I. Caraballo, M. V. de Paz and J. A. Galbis, *Polymer*, 2000, **41**, 821–826.
- 5 A. C. Roche, I. Fajac, S. Grosse, N. Frison, C. Rondanino, R. Mayer and M. Monsigny, *Cell.Mol. Life Sci.*, 2003, **60**, 288–297.
- 6 Y. H. Yun, D. J. Goetz, P. Yellen and W. Chen, *Biomaterials*, 2004, **25**, 147–157.
- 7 X. Dai, C. Dong and D. Yan, *J. Phys. Chem. B*, 2008, **112**, 3644–3652.
- 8 A. M. Granville, D. Que'mener, T. P. Davis, C. Barner-Kowollik and M. H. Stenzel, *Macromol.Symp.*, 2007, **255**, 81–89.
- 9 N. Sharon and H. Lis, *Sci. Am.*, 1993, **268**, 82–89.
- 10 M. Ambrosi, N. R. Cameron and B. G. Davis, *Org. Biomol. Chem.*, 2005, **3**, 1593–1608.
- 11 H. J. Gabius, H. C. Siebert, S. Andre, J. Jimenez Barbero and H. Rudiger, *Chembiochem.*, 2004, **5**, 740–764.
- 12 K. H. Mortell, M. Gingras and L. L. Kiessling, *J. Am. Chem. Soc.*, 1994, **116**, 12053–12054.
- 13 M. Kanai, K. H. Mortell and L. L. Kiessling, *J. Am. Chem. Soc.*, 1997, **119**, 9931–9932.
- 14 L. L. Kiessling, J. E. Gestwicki and L. E. Strong, *Curr. Opin. Chem. Biol.*, 2000, **4**, 696–703.
- 15 C. W. Cairo, J. E. Gestwicki, M. Kanai and L. L. Kiessling, *J. Am. Chem. Soc.*, 2002, **124**, 1615–1619.

- 16 M. Dhayal and D. Ratner, *Langmuir*, 2009, **25**, 2181-2187.
- 17 G. Wulff, L. Zhu and H. Schmidt, *Macromolecules*, 1997, **30**, 4533-4539.
- 18 G. Wulff, H. Schmidt and L. Zhu, *Macromol. Chem. Phys.*, 1999, **200**, 774-782.
- 19 J. Klein, M. Kunz and J. Kowalczyk, *Macromol. Chem. Phys.*, 1990, **191**, 517-528.
- 20 G. Coullerez, P. H. Seeberger and M. Textor, *Macromol. Biosci.*, 2006, **6**, 634-647.
- 21 Y. Miura, *J. Polym. Sci., Part A: Polym. Chem.*, 2007, **45**, 5031-5036.
- 22 V. Ladmiral, E. Melia and D. M. Haddleton, *Eur. Polym. J.*, 2004, **40**, 431-449.
- 23 R. Pieters, *J. Med. Res. Rev.*, 2007, **27**, 796-816.
- 24 L. L. Kiessling and J. C. Grim, *Chem. Soc. Rev.*, 2013, **42**, 4476-4491.
- 25 V. Ladmiral, E. Melia and D. M. Haddleton, *Eur. Polym. J.*, 2004, **40**, 431-449.
- 26 M. Ambrosi, N. R. Cameron, B. G. Davis and S. Stolnik, *Org. Biomol. Chem.*, 2005, **3**, 1476-1480.
- 27 S. G. Spain, M. J. Gibson and N. R. Cameron, *J. Polym. Sci. Part A: Polym. Chem.*, 2007, **45**, 2059-2072.
- 28 A. J. Varma, J. F. Kennedy and P. Galgali, *Carbohydr. Polym.*, 2004, **56**, 429-445.
- 29 D. Cunliffe, S. Pennadam and C. Alexander, *Eur. Polym. J.*, 2004, **40**, 5-25.
- 30 N. Sharon, *Biochim. Biophys. Acta*, 2006, **1760**, 527-537.
- 31 S. G. Spain and N. R. Cameron, *Polym. Chem.*, 2011, **2**, 60-68.
- 32 L. L. Kiessling, J. E. Gestwicki and L. E. Strong, *Angew. Chem. Int. Ed.*, 2006, **45**, 2348-2368.
- 33 T. K. Dam and F. C. Brewer, *Glycobiology*, 2010, **20**, 1061-1064.
- 34 A. Varki, *Glycobiology*, 1993, **3**, 97-130.
- 35 R. L. Schnaar, P. H. Weigel, M. S. Kuhlenschmidt, Y. C. Lee and S. Roseman, *J. Biol. Chem.*, 1978, **253**, 7940-7951.

- 36 S. Muthukrishnan, M. Nitschke, S. Gramm, Z. Ozyurek, B. Voit, C. Werner and A. H. E. Mueller, *Macromol. Biosci.*, 2006, **6**, 658-666.
- 37 A. T. Gutsche, P. Parsons-Wingerter, D. Chand, W. M. Saltzman and K. W. Leong, *Biotechnol. Bioeng.*, 1994, **43**, 801-809.
- 38 S. -H. Kim, T. Hoshiba and T. Akaike, *J. Biomed. Mater. Res. Part A*, 2003, **67A**, 1351-1359.
- 39 J. -Y. Wang, F. Xiao, Y. -P. Zhao, L. Chen, R. Zhang and G. Guo, *Carbohydr. Polym.*, 2010, **82**, 578-584.
- 40 R. L. Schnaar, *Anal. Biochem.*, 1984, **143**, 1-13.
- 41 Oka, J. A.; Weigel, P. H. *J. Cell Biol.*, **1986**, *103*, 1055-1060.
- 42 J. S. Lee, S. H. Kim, Y. J. Kim, T. Akaike and S. C. Kim, *Biomacromolecules*, 2005, **6**, 1906.
- 43 S. Forster and M. Antonietti, *Adv. Mater.*, 1998, **10**, 195-217.
- 44 J. Hawker and K. L. Wooley, *Science*, 2005, **309**, 1200-1205.
- 45 A. Kobayashi, A. Koyama, M. Goto, K. Kobayashi, C. -W. Chang, K. Tomita and T. Akaike, *Proc. Jpn. Acad.*, 1993, **69**, 89-94.
- 46 K. -H. Park, R. Takei, M. Goto, A. Maruyama, A. Kobayashi, K. Kobayashi and T. Akaike, *J. Biochem.*, 1997, **121**, 997-1001.
- 47 M. Dhayal, R. Kapoor, P. G. Sistla, R. R. Pandey, S. Kar, K. K. Saini and G. Pande, *Mat. Sci. Eng. C*, 2014, **37**, 99-107.
- 48 M. Dard, M. A. Sewing, J. Meyer, S. Verrier, S. Roessler and D. Scharnweber, *Clin. Oral Investig.*, 2000, **4**, 126-129.
- 49 B. Vagaska, L. Bacakova, E. Filova and K. Balik, *Physiol. Res.*, 2010, **59**, 309-322.
- 50 W. H. Chen, Y. Tabata and Y. W. Tong, *Curr. Pharm. Des.*, 2010, **16**, 2388-2394.

- 51 M. Dhayal, R. Kapoor, P. G. Sistla, C. Kant, R. R. Pandey, G. Krishnan Kumar Saini and G. Pande, *J. Biomed. Mater. Res. A*, 2012, **100A**, 1168-1178.
- 52 K. Anselme, *Biomaterials*, 2000, **21**, 667-681.
- 53 C. J. Wilson, R. E. Clegg, D. I. Leavesley and M. J. Percy, *Tissue Eng. Part A*, 2005, **11**, 1-18.
- 54 K. C. Dee and R. Bizios, *Biotechnol. Bioeng.*, 1996, **50**, 438-442.
- 55 K. Babiuch, C. R. Becer, M. Gottschaldt, J. T. Delaney, J. Weisser, B. Beer, R. Wyrwa, M. Schnabelrauch and U. S. Schubert, *Macromol. Biosci.*, 2011, **11**, 535-548.
- 56 L. A. Hidalgo-Bastida and S. H. Cartmell, *Tissue Eng. Part B*, 2010, **16**, 405-412.
- 57 A. B. Lowe, B. S. Sumerlin and C. L. McCormick, *Polymer*, 2003, **44**, 6761-65.
- 58 L. Albertin, M. Stenzel, C. Barner-Kowollik, L. J. R. Foster and T. P. Davis, *Macromolecules*, 2004, **37**, 7530-37.
- 59 N. R. Cameron, S. G. Spain, J. A. Kingham, S. Weck, L. Albertin, C. A. Barker, G. Battaglia, T. Smart and A. Blanz, *Faraday Discuss*, 2008, **139**, 359-68.
- 60 M. Sim, H. Kondo and C. H. Wong, *J. Am. Chem. Soc.*, 1993, **115**, 2260-67.
- 61 J. W. Woodcock, X. Jiang, R. A. E. Wright and B. Zhao, *Macromolecules*, 2011, **44**, 5764-75.
- 62 Z. Petrovica, S. Konstantinovic and A. Spasojevic, *Indian J. Chem. Sec. B*, 2004, 132-134.
- 63 G. Pasparakis and C. Alexander, *Angew. Chem. Int. Ed.*, 2008, **47**, 4847-50.
- 64 I. Miki, N. Ishihara, M. Otsu and H. Kase, *J. Immunol. Methods.*, 1993, **164**, 255-61.
- 65 J. S. Bauer, J. Varner, C. Schreiner, L. Kornberg, R. Nicholas and R. L. Juliano, *J. Cell Biol.*, 1993, **122**, 209-221.
- 66 H. Nathaniel and D. J. Mooney, *Nature*, 2009, **462**, 426-32.
- 67 M. P. Lutolf, F. E. Weber, H. G. Schmoekel, J. C. Schense, T. Kohler, R. Muller and J. A. Hubbell, *Nat. Biotechnol.*, 2003, **21**, 513-18.

68 J. A. Hubbell, *Nat. Biotechnol.*, 1995, **13**, 565-76.

69 Z. You, H. Cao, J. Gao, P. H. Shin, B. W. Day and Y. Wang, *Biomaterials*, 2010, **31**, 3129-38.

70 Y. Miura, *Polym. J.*, 2012, **44**, 679–689.

Scheme Caption:

Scheme 1. Schematic representation of the syntheses of glycopolymers (0, 4 and 6 indicates spacer length) *via* the RAFT process and deacetylation of the pendant 2,3,4,6-tetra-*O*-acetyl-D-glucopyranoside.

Table Caption:

Table 1 Acetylated and deacetylated glycopolymers characteristics.

Figure Captions:

Fig. 1 ^1H -NMR spectra of (a) poly(AHTAGP) in CDCl_3 and (b) **GP3** in D_2O .

Fig. 2 Osteoblast cells adhesion after 4 h at (a) without the use of glycopolymers, (b) 100 nM, (c) 1 μM , (d) 10 μM and (e) 100 μM concentrations of glycopolymers.

Fig. 3 Osteoblast cells adhesion after 4 h at (a) without the use of glycopolymer, (b) 10, (c) 100, (d) 1000, and (e) 2000 μM concentrations of glycopolymers.

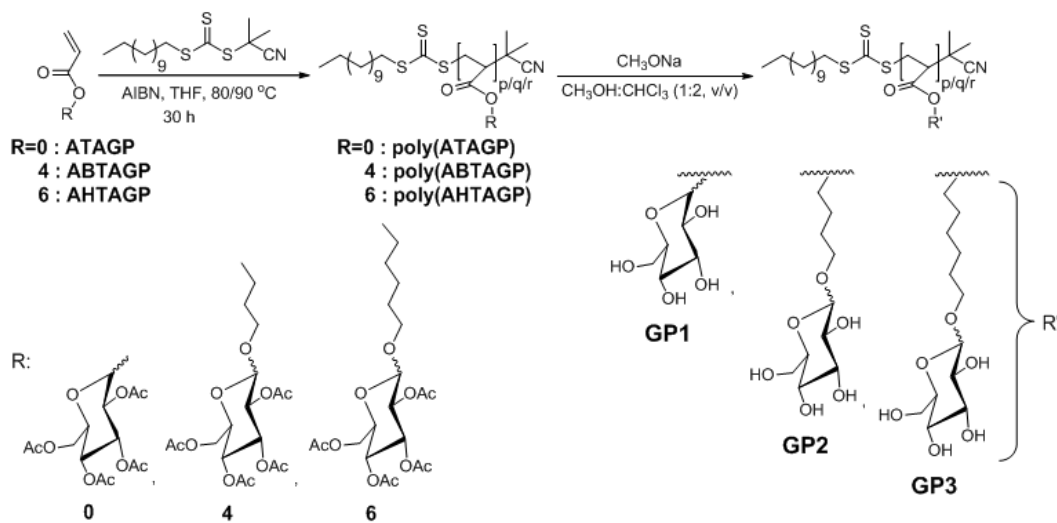
Fig. 4 Fluorescent microscopic images of osteoblast cells stained with integrin $\alpha 5$ and talin at 1 μM concentration of **GP1**, **GP2**, **GP3** and control (without the use of glycopolymer).

Fig. 5 Brightfield microscopic images of osteoblast cells (a) control (without the use of glycopolymer) and at 1 μM concentration of (b) **GP1**, (c) **GP2** and (d) **GP3**.

Fig. 6 Osteoblast cells fluorescent microscopy images of actin staining for assessing the expression of cytoskeleton protein at (a) 10, (b) 100, (c) 1000, and (d) 2000 μM concentrations of glycopolymers. Insets are magnified images.

Fig. 7 Osteoblast cells viability after 24 h at various concentrations of covalently bonded glucose moiety in glycopolymers. Cells viability values plotted in (a) logarithmic scale which highlights relatively various low concentrations and (b) normal scan which highlights response at higher concentrations. In logarithmic scale the values at 0.0001 represents cell viability without addition of the glycopolymers.

Fig. 8 Osteoblast cells proliferation at various concentrations of covalently bonded glucose moiety of glycopolymers assessed at 24, 48 and 72 h after cell plating. (a) **GP1**, (b) **GP2** and (c) **GP3** responses were plotted in logarithmic scale. In logarithmic scale the values at 0.0001 represents cell proliferation without addition of the glycopolymers. (a') **GP1**, (b') **GP2** and (c') **GP3** response were plotted in normal scale to highlight variations at higher concentrations.



Scheme 1. Schematic representation of the syntheses of glycopolymers (0, 4 and 6 indicates spacer length) *via* the RAFT process and deacetylation of the pendant 2,3,4,6-tetra-*O*-acetyl-D-glucopyranoside.

Table 1 Acetylated and deacetylated glycopolymers characteristics.

Acetylated				Deacetylated				
Polymer	GPC ^a		T _g ^b	Polymer	GPC ^a		Molecular weight ^c (cal.)	T _g ^b
	M _n	M _w /M _n	/°C		M _n	M _w /M _n		/°C
P(ATAGP)	15345	1.09	86	GP1	10829	1.15	9880	1
P(ABTAGP)	18450	1.13	97	GP2	9856	1.16	13582	4
P(AHTAGP)	10959	1.07	71	GP3	4266	1.03	7917	7

^ain DMF at room temperature, ^bfrom DSC curve on second heating, ^cmolecular weight = $M_w(\text{GPC value of acetylated glycopolymer}) - \{[M_w(\text{GPC}) - 345] \div \text{monomer molecular weight}\} \times 168$ where 345 and 168 are the macromolecular terminal ends molecular weight and total pedant acetates molecular weights.

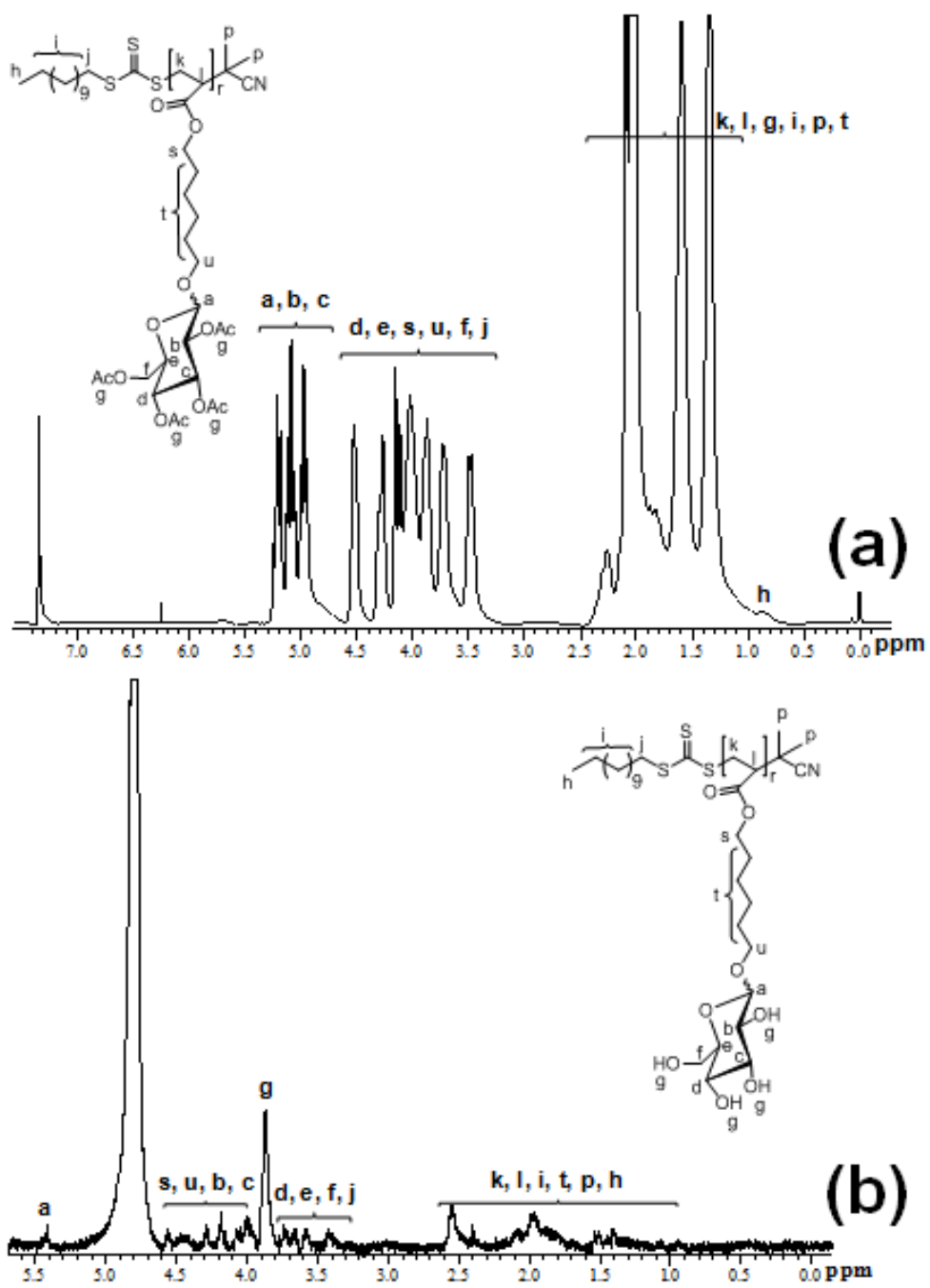


Fig. 1 $^1\text{H-NMR}$ spectra of (a) poly(AHTAGP) in CDCl_3 and (b) GP3 in D_2O .

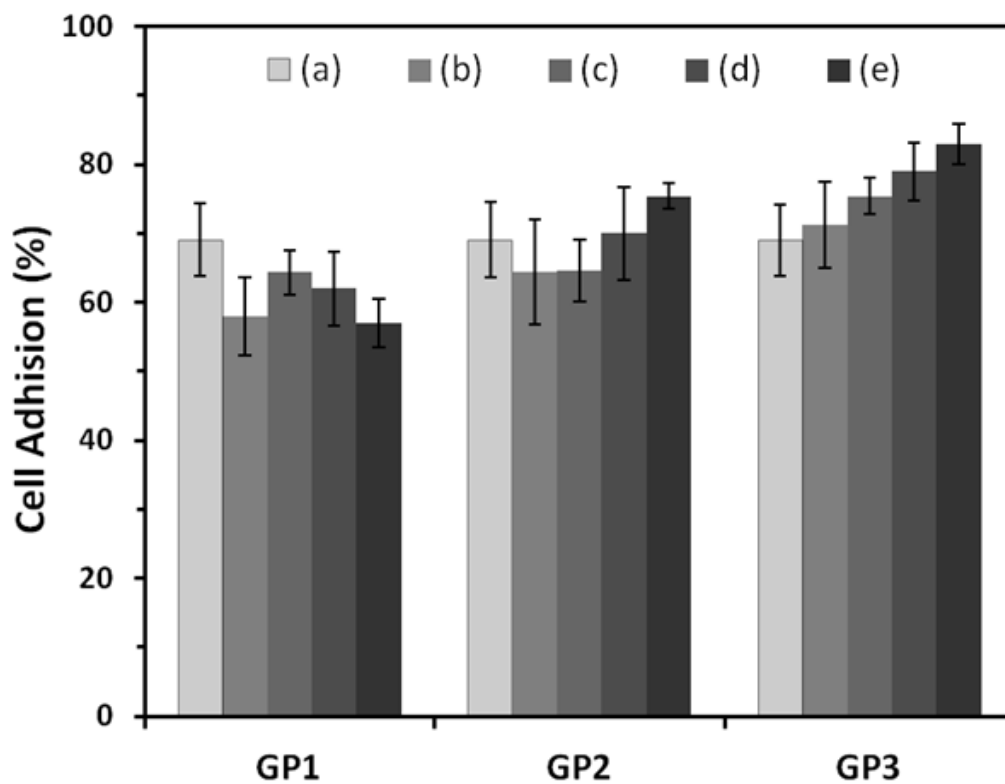


Fig. 2 Osteoblast cells adhesion after 4 h at (a) without the use of glycopolymers, (b) 100 nM, (c) 1 μM, (d) 10 μM and (e) 100 μM concentrations of glycopolymers.

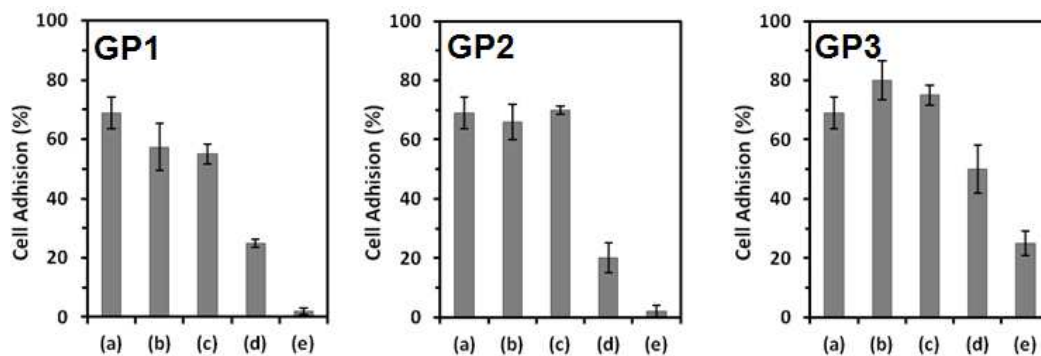


Fig. 3 Osteoblast cells adhesion after 4 h at (a) without the use of glycopolymer, (b) 10, (c) 100, (d) 1000, and (e) 2000 μM concentrations of glycopolymers.

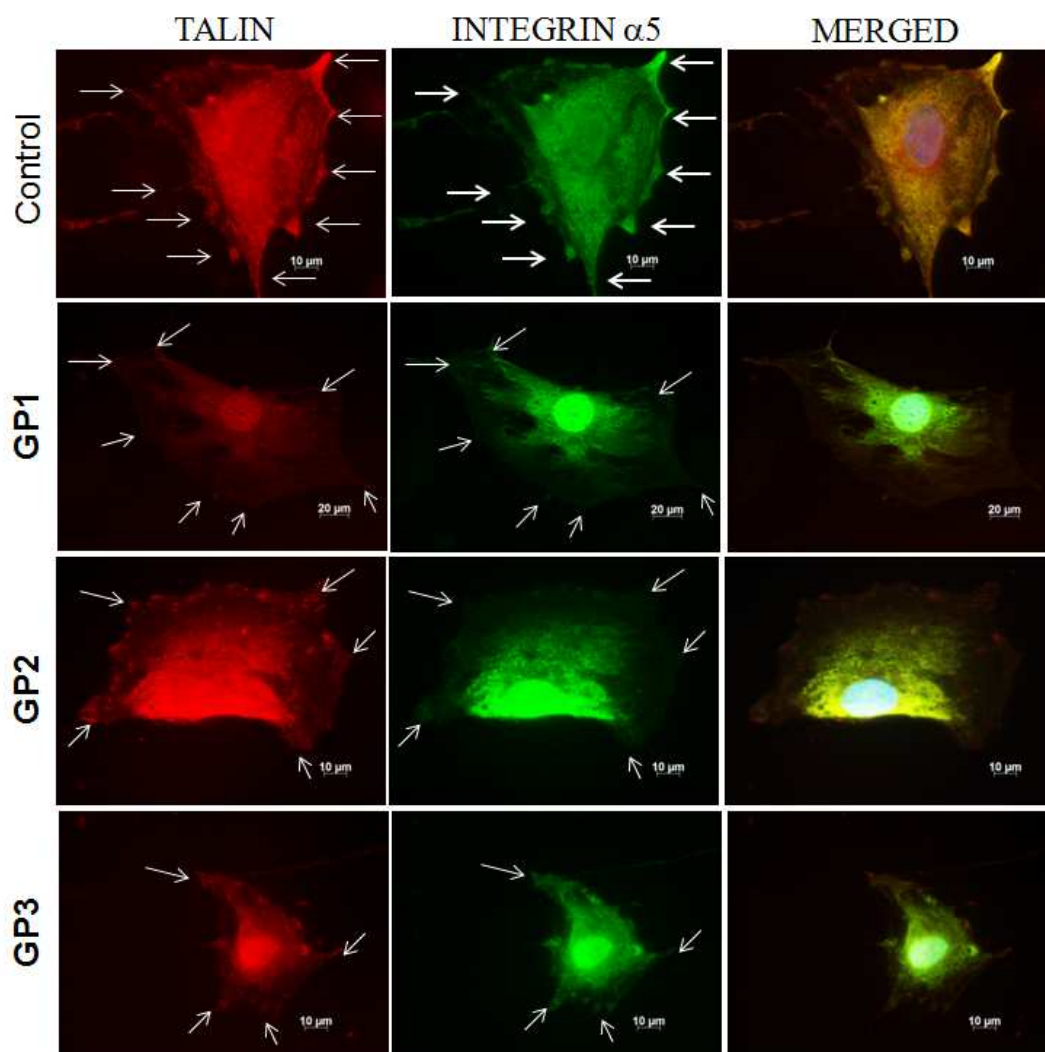


Fig. 4 Fluorescent microscopic images of osteoblast cells stained with integrin $\alpha 5$ and talin at 1 μM concentration of **GP1**, **GP2**, **GP3** and control (without the use of glycopolymer).

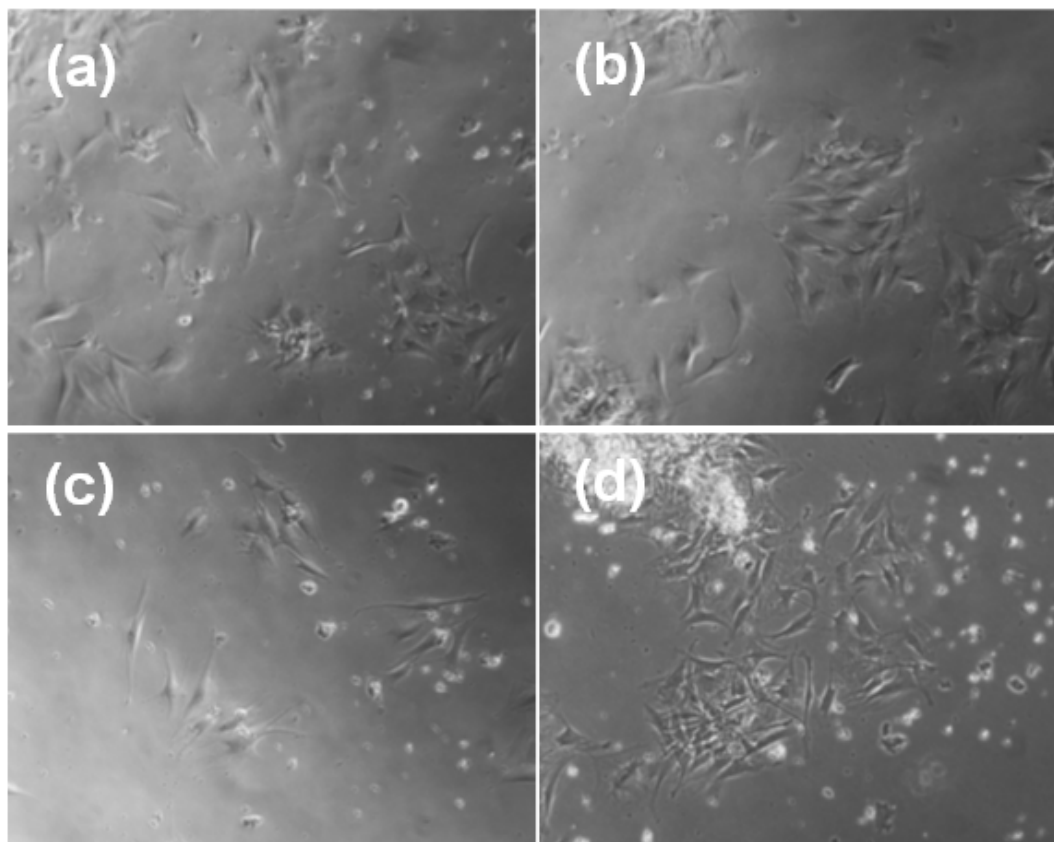


Fig. 5 Brightfield microscopic images of osteoblast cells (a) control (without the use of glycopolymer) and at 1 μM concentration of (b) **GP1**, (c) **GP2** and (d) **GP3**.

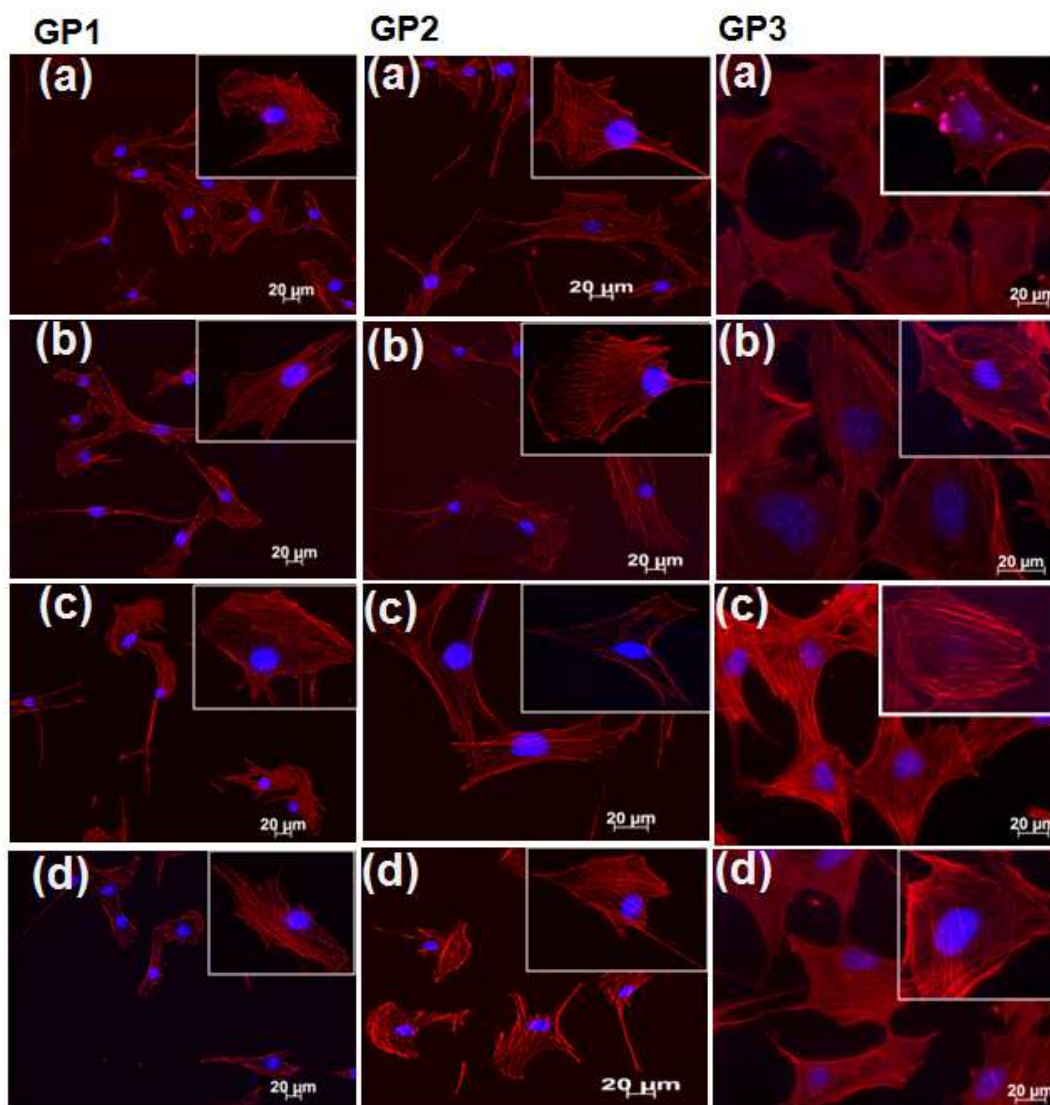


Fig. 6 Osteoblast cells fluorescent microscopy images of actin staining for assessing the expression of cytoskeleton protein at (a) 10, (b) 100, (c) 1000, and (d) 2000 μM concentrations of glycopolymers. Insets are magnified images.

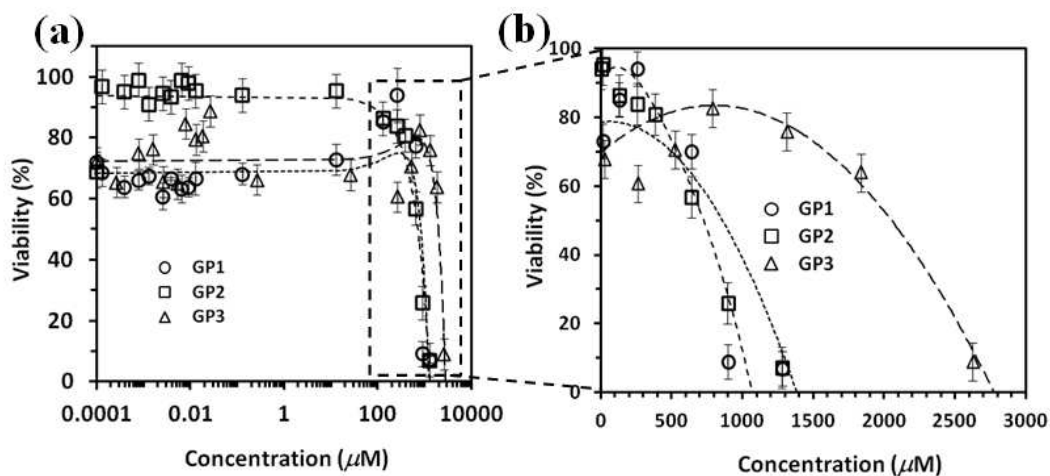


Fig. 7 Osteoblast cells viability after 24 h at various concentrations of covalently bonded glucose moiety in glycopolymers. Cells viability values plotted in (a) logarithmic scale which highlights relatively various low concentrations and (b) normal scan which highlights response at higher concentrations. In logarithmic scale the values at 0.0001 represents cell viability without addition of the glycopolymers.

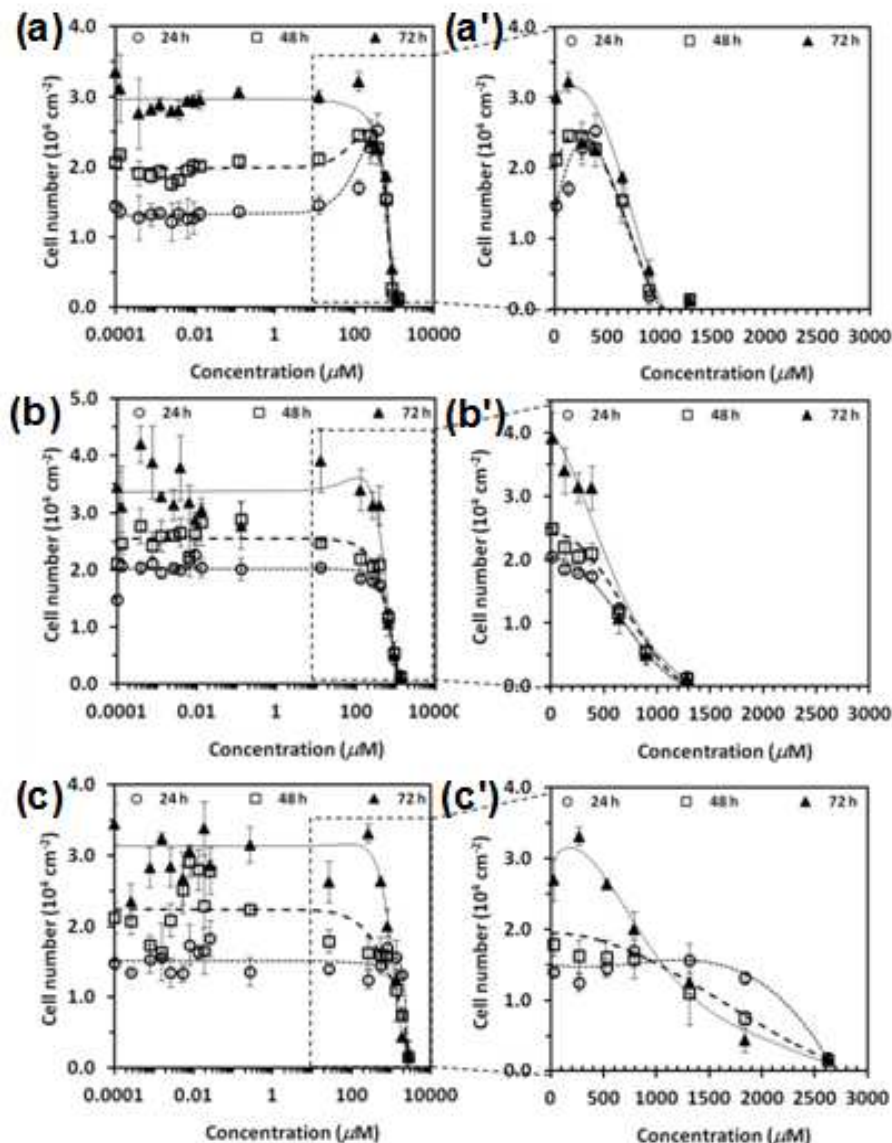


Fig. 8 Osteoblast cells proliferation at various concentrations of covalently bonded glucose moiety of glycopolymers assessed at 24, 48 and 72 h after cell plating. (a) **GP1**, (b) **GP2** and (c) **GP3** responses were plotted in logarithmic scale. In logarithmic scale the values at 0.0001 represents cell proliferation without addition of the glycopolymers. (a') **GP1**, (b') **GP2** and (c') **GP3** response were plotted in normal scale to highlight variations at higher concentrations.